24th COBEM - 2017

24th ABCM International Congress of Mechanical Engineering
December 3-8, 2017, Curitiba, PR, Brazil

COBEM-2017-1137
FLOW VISUALIZATION AND NUMERICAL INVESTIGATION OF GAP VORTEX INSTABILITY IN A RECTANGULAR CHANNEL CONTAINING A SINGLE ROD BUNDLE

Herbert Antônio Moreira Severino[1]
Jhon Nero Vaz Goulart[2]
University of Brasilia, Group of Experimental and Computacional Mechanics- GMEC, Gama, Brazil
[1]herbert.ams@gmail.com, [2]jvaz@unb.br

Alexandre Vagtinski de Paula
Federal University of Rio Grande do Sul, DEMEC, Porto Alegre, Brazil
depaula@ufrgs.br

Abstract. *Numerical simulation and flow visualization technique were employed to study the features of the turbulent flow and the large scale structure formation in a closed compound channel. The compound channel is the same geometry that was presented years ago by Guellouz and Tavoularis (2000a) which contains only one rod bundle in a rectangular main channel. However, due to the mas flow rate limitations in our experimental facilities, the Reynolds number was lowered to* $Re_{Dh} = 8000$*. The Reynolds number, for both numerical and experimental visualization, was computed from the bulk velocity,* U_b*, the hydraulic-diameter,* D_h*, and the kinematic viscosity,* ν*. As regards to the numerical methodology finite volumes were applied to discretize the domain along with the URANS* $\kappa - \omega$ *SST model to overcome the additional diffusivity caused by the turbulent motion. To shorten the computational domain periodic boundaries in streamwise direction were employed. Flow visualization was carried out by using jet ink technique to visualize the coherent structures formation in a 3 meters long channel. The rod is placed far from the upper channel's wall by a distance d. The dimensionless distance between the centre of the rod and the nearest channel's wall, W and the rod diameter, D is* W/D *- ratio 1.10. Numerical simulation presented good agreement with experimental work from Guellouz, specially for the dynamic of the turbulent flow. As regards the average quantities, these ones showed some discrepancies in comparison with the experimental outcomes published by Guellouz and Tavoularis (2000a). Such discrepancies may be attributed to the Reynolds number difference between both works. In the former work the Reynolds number, based on the same scales from our simulation, is 108000.*

Keywords: *Flow visualization, Large scale structure, Rod bundle, SST Model*

1. INTRODUCTION

Compound channels can be described as a channel whose its cross-section is characterized by the presence of adjacent subchannels connected to the main channel (Goulart, 2009). Quasi-periodic oscillation in the narrow gap is one of the most striking feature found in compound channels, does not matter if it is open or closed. Large scale motions in rod bundles are known for approximately a half century at least (Chang and Tavoularis, 2012). Rowe *et al.* (1974), were the pioneers to study the influence of the macroscopic structure of the turbulent main flow in the mixing process in a compound channel. The author worked with an rod package arranged parallel to the flow in order to determine the convective coefficients of heat transfer around the bars. The most relevant conclusion from that work was to show that the velocity signal presented a strong periodicity, implying that the coherent large scale structures dominated the gap vicinity. Furthermore, the authors also showed that the convective heat transfer coefficient was enhanced by the mixing process augmentation at the region.

Several works have been aimed to understand and predict the flow field gap oscillation over the years since then, eg. Hooper and Rehme (1984); Möller (1992); Wu and Trupp (1993); Wu and Trupp (1994); Krauss and Meyer (1998); Guellouz and Tavoularis (2000a); Guellouz and Tavoularis (2000b); Choueiri and Tavoularis (2014); Melo *et al.* (2017).Numerical works have also tried to raise awareness of the knowledge on the subject. Gosset and Tavoularis (2006), Home and Ligtstone (2014) and Derksen (2010) are noteworthy. Recently, numerical work from Ferrari and Goulart (2015) noticed that the flow field oscillation can also occurs in laminar flow state for Reynolds numbers as low as 1800. Furthermore, the authors also studied pressure drop friction factor for closed compound channels that are prone to the gap instabilities.

The friction factor was found to increase when the gap instability appeared, comparing to the friction factor computed for laminar pipe flow.

Chang and Tavoularis (2012) provided a very thorough work on gap instabilities in a rectangular channel containing one single rod. The authors carried out simulations using several turbulence models (URANS, LES and hybrid models), afterwards comparing their outcomes to the experimental work carried years ago buy (Guellouz and Tavoularis, 2000a). According to authors, LES provided the best prediction of the results compared to the other methods, however, the authors concluded that the URANS models could also be used as an cheaper alternative rather than.

Goulart *et al.* (2016) performed a numerical work based on the experimental paper developed by Meyer and Rehme (1994). The authors used the hybrid URANS/LES model, along with streamwise direction periodicity. Such alternative shortened the computational domain from 7000 mm (in the original work) to 730 mm. Both numerical procedures employed were successful to predict the dynamic of the flow and the mass flow distribution inside the channel. Moreover, based on the good agreement with the experimental paper, Goulart and co-workers showed that the streamwise periodicity can be applied to this kind of problem without any important drawback.

The objective of this work is to simulate the turbulent flow field in a closed compound channel for a low Reynolds number. As aforementioned the compound channel is the same used by (Guellouz and Tavoularis, 2000a) and (Guellouz and Tavoularis, 2000b) that contains only one single rod inside. Numerical work was developed in a commercial platform ANSYS®CFX using Unsteady Reynolds Averaged Navier-Stokes (URANS) and $\kappa - \omega$ - SST model as well. The Reynolds number, based on the bulk velocity, U_b, the hydraulic-diameter, D_h and the kinetic viscosity was computed as $Re_{Dh} = 8.0 \times 10^3$. To minimize the computational cost periodic boundary conditions were applied in streamwise direction. Such numerical procedure reduced the computational domain to $8D$, whereas the experimental work was $56D$. The computational strategy was also successfully applied for several authors e.g. Merzari *et al.* (2008), Duan and He (2017), Goulart *et al.* (2016), Gurunath (2012), Ferrari *et al.* (2016), Home *et al.* (2009), Home and Ligtstone (2014), Derksen (2010).

Flow field visualization was also carried out in this work. Jet ink technique was employed to observe the gap instability formation on slice between the rod's surface and the upper channel's wall, Fig. 1b. Both numerical results and the flow visualization were compared to the experimental outcomes published by Guellouz and Tavoularis (2000a).

2. EXPERIMENTAL PROCEDURE

The experiments were conducted in a closed channel in steady state regime. Water at room temperature ($\approx 25\ ^\circ C$) was used as work fluid. The work fluid was driven by a centrifugal pump in closed loop. The compound channel's test section is constant being width $L = 193\ mm$, height $H = 151\ mm$ measuring $L_t = 3290\ mm$, meters long. In terms of rod diameter is $L = 3.3D$, $H = 2.5D$ and $L_t = 54.8D$. A thorough schematic view of the channel is presented in Fig. 1a and 1b.

The fluid reaches the test section, after passing through a diffuser and a set of honeycombs. The test section contains one single rod with external and internal diameter $D = 60mm$, and the length $L_s = 2000\ mm$ ($L_s = 33.3D$). The rod is far from upper channel wall by a distance W, which produces W/D- ratio that matches with test section studied Guellouz and Tavoularis (2000a). In this paper both dimensionless parameters, W/D-ratio and Reynolds number were kept constant throughout the work, 1.10 and 8000, respectively.

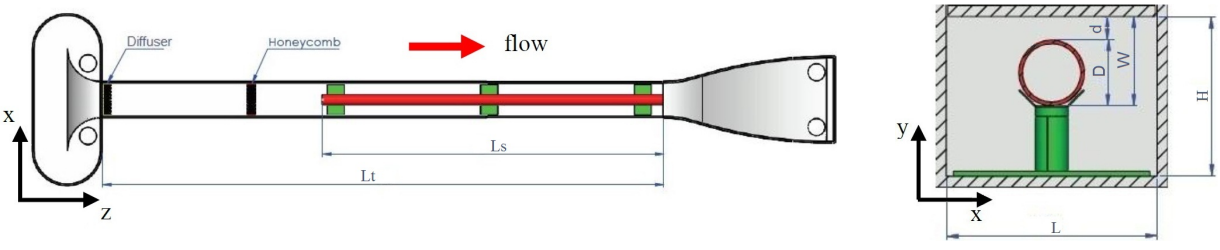

(a) (b)

Figure 1: Sketch of the flow facility.(a) Upper view; (b) Inside section view

The Reynolds number was calculated with velocity bulky U_b, hydraulic diameter D_h and kinematic viscosity, ν, according to Eq. 1. The volumetric flow rate was controlled by a frequency inverter which controls two centrifugal pumps of $1/2CV$ each. The bulk velocity, was than computed $U_b = 0.074\ m/s$. Flow visualization employed ink jet technique that was released upstream the honeycomb in order to obtain linear fillets of ink. Such care ensures that the observed disturbances were coherent structures those are formed only due to geometry. The hydraulic diameter was computed $D_h = 109\ mm$ leading to a dimensionless length $L = 18.3D_h$.

$$Re_{Dh} = \frac{U_b\, D_h}{\nu} \rightarrow D_h = \frac{4\, A}{P} \tag{1}$$

In Eq. 1 A is cross section area and P is wet perimeter of the test section.

3. CFD METHODOLOGY

3.1 Geometry and flow conditions

The computational domain is depicted in Fig. 2a and 2b, being the same geometry where the flow visualizations were performed. It consists in a single cylindrical rod, $D = 60\ mm$, placed a rectangular channel with width $Lx = 3.3D$ and $Ly = 2.5$. The only difference compare to the experimental facility lies in the fact that the channels length is shorter than our experimental facility. The original length of the channel was significantly shortened to length $Lz = 480\ mm$ ($Lz = 8D$), through the streamwise periodicity adoption, Fig. 2a. The mass flow rate was calculated based on the experimental work, Fig. 1, and it was kept constant, $\dot{m} = 1.95\ Kg/s$. The gap size, between the rod and upper wall of channel is $d = 6\ mm$, yielding W/D - ratio 1.10, therefore. At the walls the velocity was imposed null. Neither heat flux nor the specific water mass, ρ, were allowed to change during the numerical computations.

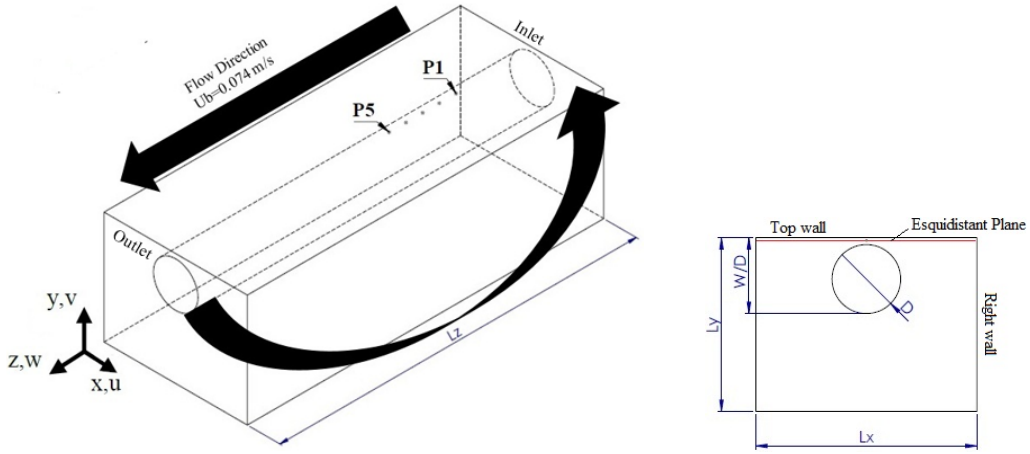

(a) (b)

Figure 2: (a) Schematic view of computational domain. (b) Channel's cross-section and its dimensions.

3.2 Mesh strategy and mesh independence

In order to determine the length of the domain in the main direction a study mesh independence was carried out. Different length domains were evaluated, $Lz = 360\ mm$, $480\ mm$, $720\ mm$ ($Lz/D = 6$, 8 and 12). For the first one, $Lz/D = 6$, it was not possible to solve the mass balance in good accuracy as we expected. For the computational domains $8D$ and $12D$ there was no significant dynamic variation of the flow. So, we chose the smaller one, $Lz/D = 8$.

All meshes were discretized with hexahedral volumes, by splitting up the computational domain into smaller ones. In the upper channel's wall and rod wall the mesh was refined to obtain a $y^+ < 1$. In the other walls of the cross section a refinement was applied yield $y^+ \approx 10$. In streamwise direction z^+ was chosen to be about 25. Fig. 3a shows the mesh used in a cross-section. It should be noticed the mesh refinement near the top wall and around the tube.

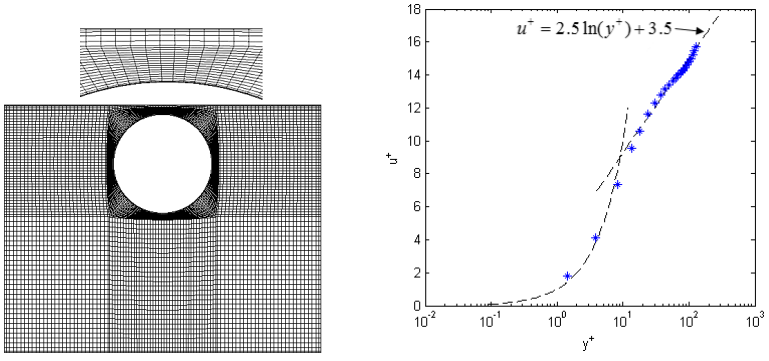

(a) (b)

Figure 3: (a) Computational mesh in the cross-section. (b) Law of the wall obtained at the rod surface.

The whole simulation was performed with a time step equivalent to $0.005\ s$, with the Courant- Friedrichs- Lewy

$CFL_{max} \approx 0.35$.

In Fig. 3b the good quality of the numerical simulation and the mesh can be observed. The velocity near the rod surface is plotted as a function of y^+. From the Fig. 3b we see that the mesh was able to describe in a good way the subviscous layer, that is required by $\kappa - \omega$ - SST model. In addition, the classic wall function was practically recovered.

4. SST MODEL FORMULATION

The SST model was proposed by Menter (1994). In this model, the formulation of the $k-\varepsilon$ model is used far from the wall region and near the wall is applied $k-\omega$ model. The zonal formulation is based on blending functions, which ensure a proper selection of the $k-\varepsilon$ and $k-\omega$ zones. The basic formulation of the incompressible continuity and Navier-Stokes equations are

$$\frac{\partial \overline{u_i}}{\partial x_i} = 0 \tag{2}$$

$$\frac{\partial \overline{u_i}}{\partial t} + \frac{\partial \overline{u_i u_j}}{\partial x_j} = -\frac{1}{\rho}\frac{\partial \overline{p}}{\partial x_i} + \nu \frac{\partial^2 \overline{u_i}}{\partial x_j^2} + \frac{\partial \tau_{ij}}{\partial x^j} = 0 \tag{3}$$

The complete formulation of the SST model is given, with the limited number of modifications highlighted.

$$\frac{\partial(\rho k)}{\partial t} + \frac{\partial(\rho U_i k)}{\partial x_i} = P_k - \beta^* \rho k\omega + \frac{\partial}{\partial x_i}\left[(\mu + \frac{\mu_t}{\sigma_k})\frac{\partial k}{\partial x_i}\right] \tag{4}$$

$$\frac{\partial(\rho \omega)}{\partial t} + \frac{\partial(\rho U_i \omega)}{\partial x_i} = \alpha \rho S^2 - \beta \rho \omega^2 + \frac{\partial}{\partial x_i}\left[(\mu + \frac{\mu_t}{\sigma_\omega})\frac{\partial \omega}{\partial x_i}\right] + 2(1-F_1)\rho\sigma_{\omega 2} + \frac{1}{\omega}\frac{\partial k}{\partial x_i}\frac{\partial \omega}{\partial x_i} \tag{5}$$

The turbulence eddy viscosity is defined as follows:

$$\nu_t = \frac{\alpha_1 k}{\max(\alpha_1 \omega, (SijSij)^{\frac{1}{2}} F_2)} \tag{6}$$

Where S is the invariant measure of the Strain Rate. The blending function is based on the distance to the nearest surface on the flow variables

$$F_1 = \tanh(arg_1^4) \tag{7}$$

$$arg_1 = \min\left[\max\left(\frac{\sqrt{k}}{\beta^*\omega}, \frac{500\nu}{y^2\omega}\right), \frac{4\rho\sigma_{\omega 2} k}{CD_{k\omega} y^2}\right] \tag{8}$$

with $CD_{k\omega}$ is defined for Eq. 9 and y is the distance to the nearest wall. F_1 is equal to zero away from the surface ($k-\varepsilon$ model), and switches over to one inside the boundary layer ($k-\omega$ model).

$$CD_{k\omega} = \max(2\rho\sigma_{\omega 2}\frac{1}{\omega}\nabla k \nabla \omega, 1, 0.10^{-10}) \tag{9}$$

F_2 is a second blending function defined by:

$$F_2 = \tanh(arg_2^2) \tag{10}$$

$$arg_2 = \max\left(\frac{2\sqrt{k}}{\beta^*\omega y}, \frac{500\nu}{y^2\omega}\right) \tag{11}$$

A production limit used in the SST model to prevent the rise of turbulence in stagnation regions:

$$P_k = \mu_t \frac{\partial U_i}{\partial x_j}\left(\frac{\partial U_i}{\partial x_j} + \frac{\partial U_j}{\partial x_i}\right) \rightarrow \tilde{P_k} = \max(P_k, 10 \cdot \rho\beta^* k\omega) \tag{12}$$

All constants are computed by a blend from the corresponding constants of the $k-\varepsilon$ model and $k-\omega$ model via $\alpha = \alpha_1 F_1 + \alpha_2(1-F_1) + \ldots$. The constants for this model are $\beta^* = 0.09$, $\alpha_1 = 5/9$, $\beta_1 = 0.075$, $\sigma_{k1} = 0.85$, $\sigma_{\omega 1} = 1/2$, $\alpha_2 = 0.44$, $\beta_2 = 0.0828$, $\sigma_{\omega 2} = 0.856$, $\sigma_{k2} = 1$.

5. RESULTS AND DISCUSSION

5.1 Mean velocity Distribution

In Fig. 4 the time-average isocontours of the streamwise velocity is showed along with the results published year ago by Guellouz and Tavoularis (2000a). The data were gathered in the middle of the computational domain at $Lz/D = 4$, being stressed in dimensionless form by the bulk velocity, U_b. All quantities were averaged over a time $t = 16T_c$, where T_c is the convective time, $T_c = L_z/U_b$. In general form $\kappa - \omega$ SST was able to capture some remarkable features of the mass flow rate distribution in this kind of compound channel. Numerical methodology was able to predict the very well pronounced bulging of the isolines towards the edges arisen from the secondary flows according to Meyer (2010). In a qualitative way both velocity maps are in good agreement despite the Reynolds number difference. The maximum axial velocity is W/U_b was found about 1.20 taking place at the main subchannel. At the same location Guellouz and Tavoularis found $W/U_b = 1.17$, (Fig. 4 (a) and (c)). However, the mass distribution has found its strongest discrepancy near to the narrow gap. The zone at the gap was magnified, Fig. 4 (b), to provide a better comparison with Guellouz's experiment. There we can see quite similar isoline patterns in both works, however, our values seemingly are scaled by a factor of 0.5 in comparison to the experimental work. Such discrepancy may be attributed to Reynolds difference between numerical and experimental works, 8000 and 108000, respectively.

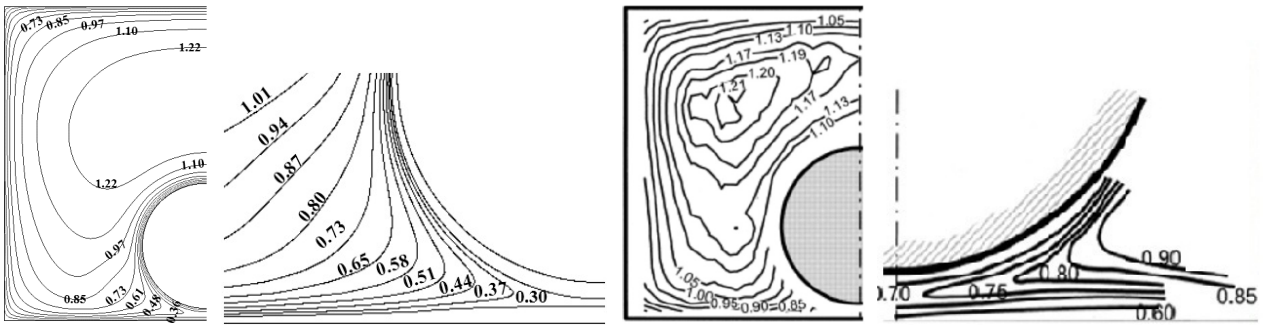

(a) (b) (c) (d)

Figure 4: Isolines of streamwise velocity components. (a) and (b) present work. (c) and (d) work from Guellouz and Tavoularis (2000a).

5.2 Kinetic Energy Distribution

In the same way Fig. 5 shows the isolines patterns the kinetic energy inside the channel. The data were gathered at the same location, $Lz/D = 4$, and averaged over the same aforementioned time. Data are also stressed in dimensionless form $k^* = k/U_b^2$. Although there is a remarkable difference between both Reynolds number, the numerical and experimental results are in good agreement, mainly far from the gap region. Near the lateral wall the numerical code predicted k^* about 0.012, whereas the experimental map shows 0.01. Again, the difference really matters when the turbulent quantities are analysed at gap vicinity. The prediction of k^* at this region was found lowered in one order when compared to the experimental work. It is worth to mention that the Reynolds number for numerical computation is also one order lower than experimental work carried out by Guellouz and Tavoularis (2000a), so such difference may attributed by the Reynolds number.

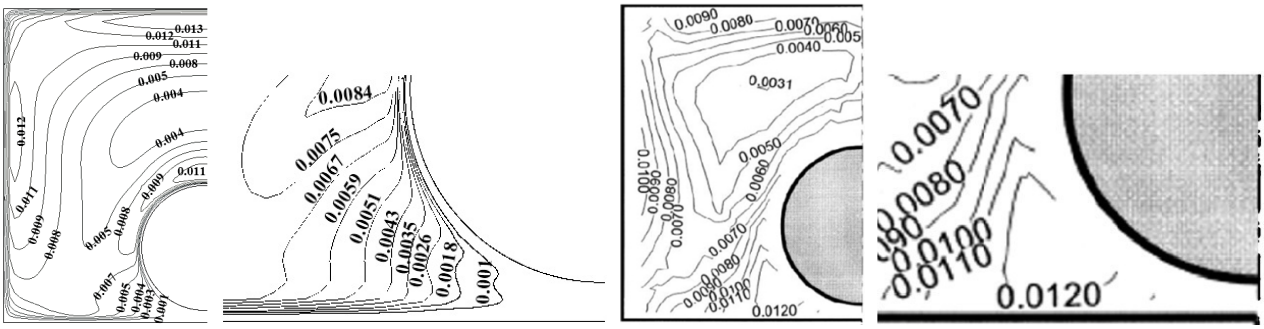

(a) (b) (c) (d)

Figure 5: Isocontours of average turbulent kinetic energy. (a) and (b) present simulation. (c) and (d) experimental work from Guellouz and Tavoularis (2000a).

5.3 Coherent structures characterization

One of the most striking characteristic of the turbulent flow in compound channels are the quasi-periodic flow patterns of the velocity time-traces. The periodicity of the flow field suggests the presence of large scale coherent structures in the flow. Such velocity pattern (and therefore coherent structures) is responsible for heat, mass and momentum exchanging between adjacent sub channels throughout the narrow gap. Such behavior implies, for instance, in the convective heat coefficient enhancement as well as the local mixing rates. Quasi-periodic flow was also found in laminar flow-state with Reynolds number ranging from 900 up to 1800 (Ferrari and Goulart, 2015).

Fig. 6 shows the velocity time-traces for streamwise direction. The results are made non-dimensional by the bulk velocity, U_b. The velocity time-traces were gathered at the middle gap, between the rod and bottom wall, at the position $L_x/D = 4$.

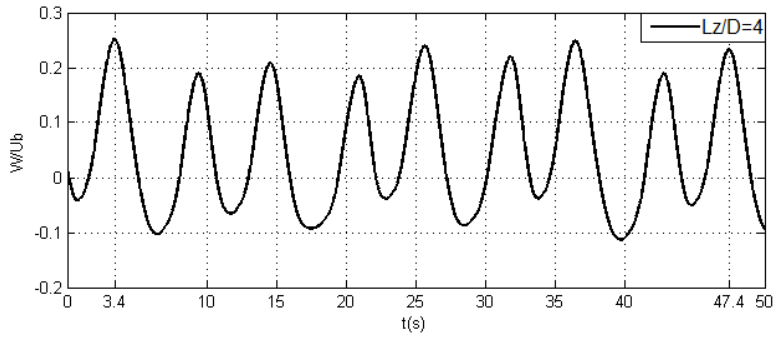

Figure 6: Streamwise velocity time-history component.

It can be seen that both velocity components show the existence of quasi-periodic behaviour inside the gap. Such characteristic is in fair agreement with the experimental works form Goulart and co-works among other researches as Möller (1992), Meyer and Rehme (1994), Meyer and Rehme (1995); Goulart *et al.* (2013), Souza *et al.* (2014), Goulart *et al.* (2016), Ferrari and Goulart (2015), Melo *et al.* (2017).

Through temporal auto-correlation the main frequency associated to the dynamic of the large motion was then determined. Auto-correlation was computed as follow,

$$Coeff_{ww}(\Delta z, \Delta t) = \frac{w'(z,t)w'(z+\Delta z, t+\Delta t)}{\overline{w'^2}(z,t)} \tag{13}$$

Fig. 7 shows the auto-correlation coefficient for streamwise velocity fluctuation component. The velocity fluctuation signal was taken at the middle gap, $L_z/D = 4$ and in some regions away from the gap ($Lz/D = 4.40$ and 4.8, points P3, P4 and P5 in Fig. 2a).

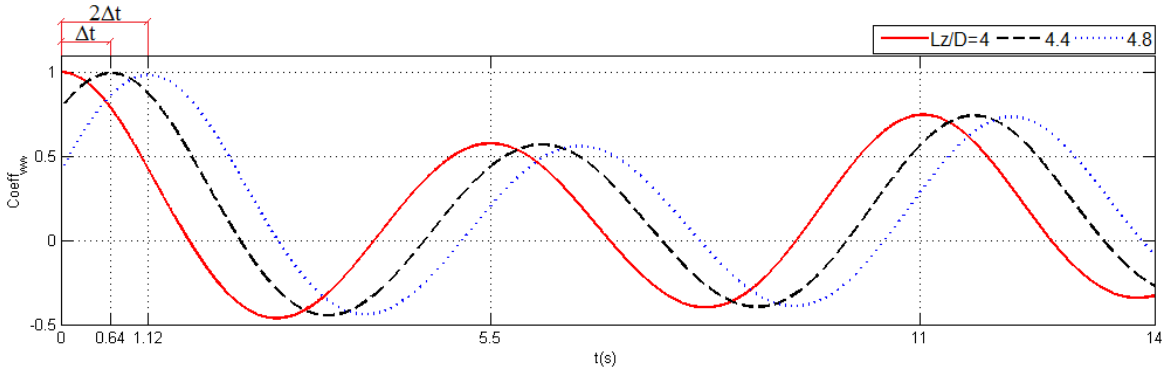

Figure 7: Auto-correlation and cross-correlation coefficients for streamwise velocity fluctuation component.

First of all, the fundamental frequency calculated through the auto-correlation was found $f = 0.182\ Hz$, regardless the distance from the channel's inlet. In order to compare the dynamic of the large motion we make the frequency dimensionless as proposed year ago by Guellouz and his co-worker (Guellouz and Tavoularis, 2000a). The Strouhal number can be written as follow,

$$S_t = \frac{f\ D}{U_b} \tag{14}$$

where, f is the main frequency attributed to the large periodic motions, Hz, D is rod's diameter, m, and U_b, is the velocity bulk.

At that time the experimental results for the same geometry and W/D - ratio produced $S_t = 0.17$, according to the authors. Based on the same scales used by the authors we calculated the Strouhal number of the numerical results, that was found S_{tn} = 0.15. Such value was quite similar to that one published years ago by the authors, despite the Reynolds number difference. It is important to remind the reader that the Reynolds number for experimental work is 108000, and, therefore, one order greater than ours, 8000. This result suggests that the dynamic of the flow is slightly affected by the Reynolds number which, in some degree, corroborates with Melo's work (Melo *et al.*, 2017). The experimental work published recently by Melo showed that the Strouhal number value is much more affected by the geometry of the compound channel, the geometric characteristic of the narrow gap and the channel's length than the Reynolds number itself. The gap width and the channel's length were found to play a very important role in the large vortices appearance and the spectral detection in the time-trace velocities as well.

We furthered our analysis by estimating the convective velocity, U_c and the wavelength number, λ, of the large vortices. Both characteristics were estimated through the velocity time series. The convective velocity is the velocity which the large vortices travel downstream the flow. It can be computed from the Eq. 15, which computes the cross-correlation coefficient between a fixed point at $Lz/D = 4$ and another point downstream, apart from each other by a distance Δz. The velocity time-histories must be gathered at the once in different locations. From Fig. 7 we can see that the signals are delayed with respect each other, suggesting that the event that happens at a certain location and time ($z = 0; t = 0$), takes some time, Δt, to take place in another position $z + \Delta z$. So, the convective velocity is then computed,

$$U_c = \frac{\Delta z}{\Delta t} \tag{15}$$

The convective velocity was then calculated and is presented as a function of bulk velocity yielding $U_c/U_b = 0.51$. Such value is lower than showed in the experimental work from Guellouz in 2000. According to the authors it should be about 0.78. However, the reader must take into account that the Reynolds number of the experimental work is one order greater than the present work and any direct comparison should be carefully evaluated. Furthermore, the dynamic characterization of the turbulent flow in this kind of geometry still needs reliable values for such Reynolds number range.

From the computed Strouhal number, S_{tn}, and the convective velocity, U_c, the wavelength, λ could also be determined as follow

$$\lambda = \frac{U_c}{f} \tag{16}$$

The wavelength, λ is the distance between two vortices whose their rotation is the same (clock or counter clockwise). In the present work the numerical code predicted $\lambda/D = 3.6$. This number is slighted lower than published by Guellouz in 2000 whose experimental work showed $\lambda/D = 4.2$.

5.4 Ink Jet Visualization

Ink jet technique was applied to visualize the flow pattern inside the gap, Fig. 8a and 8b. The screenshots were captured by a regular digital camera, since the velocity was very low. A needle containing ink was placed $10D$ upstream the compound channel's entrance. The ink is then released towards the gap in order to show the flow pattern in that region. After some distance downstream the channel, nearly $6D$, the ink showed a sinusoidal behavior indicating that the large motion has then appeared for the first time. In the Fig. 8a, 8b, experimental and numerical works are stressed along with Fig. 8c, form the experimental work carried out by Guellouz and Tavoularis (2000a) at Re_{Dh} = 16000 and W/D - ratio 1.10. Quantitatively, we cannot say anything on the flow quantities similarities between numerical and experimental works, since our experiment was not aimed to provide us such information. However, there is a striking resemblance between numerical and experimental works (present and that one from Guellouz and Tavoularis (2000a)). The ink seems to wander about the gap almost penetrating into the main subchannels.

Just before the first gap instability appearance the flow field is aligned to the rod axis, so none spanwise velocity component can be detected, and therefore, there is no (or at least unimportant) mixing between adjacent subchannels. When the gap instability starts a strong spanwise velocity component arises, as we can see in the three images from Fig. 8, promoting mass, heat and momentum exchanging between both subchannels thorugh the narrow gap. Form the ink concentration we can observe that amplitude of the "waves" is rod diameter size.

Despite the great observation we are surprised. It was expected that the sinusoidal patterns were observed farther downstream than they appeared for the first time. Furthermore, an attempt to characterize the dynamic of the flows was done from the information in the screenshots. A roughly evaluation of main frequency, wavelength and convective velocity was done then. None of them was found in good agreement with either numerical or experimental works. Such fact suggests that the pattern of the flow inside the gap may change as the flow evolves downstream the channel. However, we did not perform any kind of study to answer this question. The flow dynamic changes along the compound channel has

been recently studied by Choueiri and Tavoularis (2014) and Melo *et al.* (2017). In both works the authors showed that the main characteristics of the dynamic of the flow, such as, the main frequency, the convective velocity and the wavelength keeps some relationship with the channel's length, and therefore, is also ruled by the flow state.

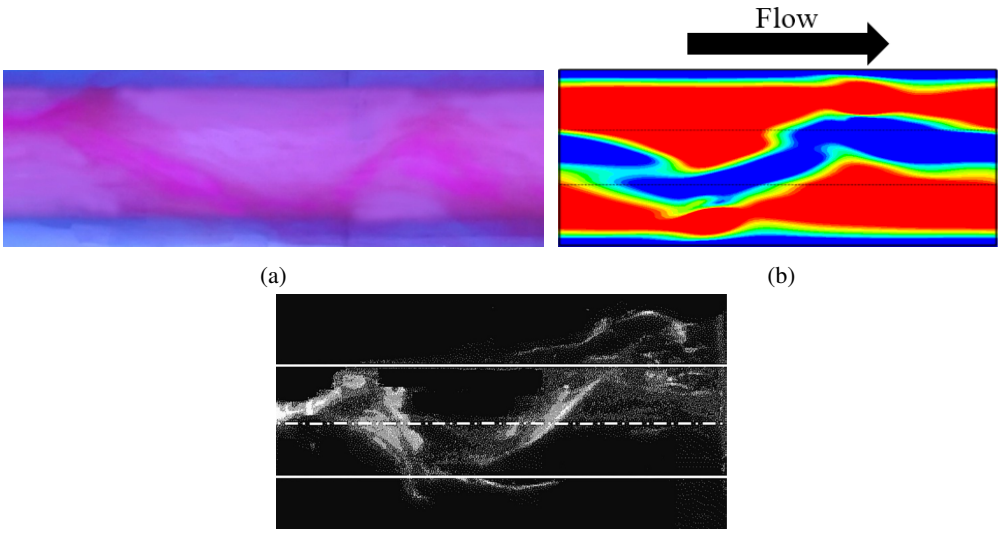

Figure 8: Flow field visualization. (a), (b) Experimental and numerical works form the present paper. (c) Visualization performed by Guellouz and Tavoularis (2000a)

6. CONCLUSION

A numerical platform was used to simulate the average and dynamic features of the turbulent flow in a closed compound channel along with experimental visualization of the flow. For both works the Reynolds number was about 8000. The numerical data were compared, as much as possible, with the results released by Guellouz and Tavoularis (2000a), who carried out an experimental work on the same topic and using similar geometry. Despite the similarities the former authors run their experiments under a Reynolds number 108000. The present work computed the Reynolds number based on the same scales used for Guellouz and Tavoularis (2000a).

Mean average quantities were predicted by $\kappa - \omega$ SST satisfactorily. Numerical results on mean axial velocity and turbulent kinetic energy were found in good agreement in comparison with experimental data from (Guellouz and Tavoularis, 2000a), despite de Reynolds number difference. However, some discrepancy could be observed. The strongest difference between both results was concentrated at the gap region. At that region both mean axial velocity and the turbulent kinetic energy were found lower than the experimental work from Guellouz. As regards the last one, this was predicted k^*=0.001 as the experimental work showed k^*=0.012. On the other hand, good predictions were achieved for the dynamic characteristics of the turbulent flow in the narrow gap. The flow visualization showed a sinusoidal velocity pattern at the gap given rise to the strong spanwise velocity component. Furthermore, both numerical and experimental visualization match in a good way.

The Strouhal number, S_{tn}, the wavelength, λ and the dimensionless convective velocity, U_c/U_b, were found in fair agreement with the experimental results, despite the Reynolds number difference. Among these three characteristics the worst case was the predicted convection velocity that was found U_c/U_b = 0.51 in our numerical simulation. The experimental work carried out by Guellouz yielded U_c/U_b about 0.78. The different agreement between the numerical and experimental results for static and dynamic flow field, lead us to conclude that the Reynolds number seems to affect the flow in different ways. As regards to the average quantities, velocities and turbulent kinetic energy, these ones seems to be affected much more than the dynamic motion is affected. However, as mentioned before reliable data for this range of Reynolds number is still necessary for a good comparison.

7. ACKNOWLEDGEMENTS

The authors would like to acknowledge the financial support provided by Fundação de Apoio a Pesquisa do Distrito Federal- FAP/DF.

8. REFERENCES

Chang, D. and Tavoularis, S., 2012. "Identification of coherent structures in axial flow in a rectangular channel containing a rod". *Nuclear Engineering and Design*, Vol. 243, pp. 176–199.

Choueiri, G.H. and Tavoularis, S., 2014. "Experimental investigation o flow development and gap vortex street in an eccentric annular channel. Part 1. Overview of the flow structure". *J. Fluid Mech*, Vol. 752, pp. 521–542.

Derksen, J.J., 2010. "Simulation of lateral mixing in cross-channel flow". *Computer and Fluids*, Vol. 39, pp. 1058–1069.

Duan, Y. and He, S., 2017. "Large eddy simulation of a buoyancy-aided flow in a non-uniform channel-Buoyancy effects on large flow structures". *Nuclear Engineering and Design*, Vol. 312, pp. 191–204.

Ferrari, J.M., Severino, H. and Goulart, J., 2016. "Determinação numérica da perda de carga e fator de atrito em canais compostos". In *Congresso Nacional de Engenharia Mecânica - CONEM2016*. Fortaleza, Brazil.

Ferrari, J.M.S. and Goulart, J.N.V., 2015. "Simulação numérica do escoamento laminar em um canal complexo". *Revista Interdisciplinar de pesquisa em engenharia*, Vol. 1.

Gosset, A. and Tavoularis, S., 2006. "Laminar flow instability in a rectangular channel with a cylindrical core." *Phys. Fluids*, Vol. 18, p. 044108.

Goulart, J., Wissink, J.G. and Wrobel, L.C., 2016. "Numerical simulation of turbulent flow in a channel containing a small slot". *Inter Journal of heat and fluid flow*, Vol. 61, pp. 343–354.

Goulart, J.N.V., Anflor, C.T.M. and Möller, S.V., 2013. "Static and dynamic characteristics of turbulent flow in a closed compound channel." *Rev. Fac. Ing. Univ. Antioquia*, Vol. 68, pp. 124–135.

Goulart, J.V.N., 2009. *Análise experimental de escoamentos cisalhantes em canais compostos fechados*. Ph.D. thesis, University Federal of Rio Grande do Sul, Brazil.

Guellouz, M.S. and Tavoularis, S., 2000a. "The structure of the turbulent flow in a rectangular channel conteining a single rod-Part 1: Reynolds-Average measurements". *Exp Thermal and Fluid Science*, Vol. 23, pp. 59–73.

Guellouz, M.S. and Tavoularis, S., 2000b. "The structure of the turbulent flow in a rectangular channel conteining a single rod-Part 2: phase-averaged measurements." *Exp Thermal and Fluid Science*, Vol. 23, pp. 75–91.

Gurunath, S.K., 2012. *Numerical Investigation of Coherent Structures in Axial Flow in Single Rod-Channel Geometry*. Master's thesis, Delft University of Technology, The Netherlands.

Home, D., Arvanitis, G. and abd M S Hamed, M.F.L., 2009. "Simulation of flow pulsation in a twin rectangular sub-channel geometry using unsteady reynolds averaged navier-stokes modelling". *Nuclear Engeenering Design*, Vol. 239, pp. 2964–2980.

Home, D. and Ligtstone, M.F., 2014. "Numerical investigation of quasi-periodic flow and vortexstructure in a twin rectangular shbchannel geometry using deched eddy simulation". *Nuclear Engeenering Design*, Vol. 270, pp. 1–20.

Hooper, J.D. and Rehme, K., 1984. "Large-scale structural effects in developed trubulent flow through closely-spaced rod arrays." *Journal Fluid Mech.*, Vol. 145, pp. 305 – 337.

Krauss, T. and Meyer, L., 1998. "Experimental investigation of turbulent transport of momemtum and enerfy in a heated rod bundle". *Nuclear Eng. Des.*, Vol. 180, pp. 185 – 206.

Melo, T., Goulart, J., Anflor, C.T. and Santos, E., 2017. "Experimental investigation of the velocity time-traces of the turbulent flow in a rectangular channel with a lateral slot." *European Journal of Mechanics B/Fluids*, Vol. 62, pp. 130–138.

Menter, F.R., 1994. "Simulation of lateral mixing in cross-channel flow". *AIAA Journal*, Vol. 32, pp. 1598–1605.

Merzari, E., Ninokata, H. and Baglietto, E., 2008. "Numerical simulation of flows in tight-lattice fuel bundles". *Nuclear Engineering*, Vol. 238, pp. 1703–1719.

Meyer, L., 2010. "From discovery to recognition of periodic large scale vortices in rod bundles as source of natural mixing between subchannels âĂŤ a review". *Nuclear Engineering and Design*, Vol. 240, pp. 1575 – 1588. ISSN 0029-5493.

Meyer, L. and Rehme, K., 1994. "Large-scale turbulence phenomena in compound rectangular channels". *Exp. Thermal Fluid Sci*, Vol. 8, pp. 286–304.

Meyer, L. and Rehme, K., 1995. "Periodic vortices in flow though channels with longitudinal slots or fins". In *10th Symposium on Turbulent Shear Flows*. The Pennsylvania State University Park August 14-16.

Möller, S.V., 1992. "Single-phase turbulent mixing in rod bundles". *Exp. Thermal and Fluid Science*, pp. 26–33.

Rowe, D.S., Johnson, B.M. and Knudsen, J.G., 1974. "Implications Concerning Rod Bundle Crossflow Mixing Based on Measurements of Turbulent Flow Structure". *Int J Heat Mass Transfer*, Vol. 17, pp. 407–419.

Souza, S.I.S., Cestaro, H.A.M. and Goulart, J.N.V., 2014. "Numerical investigation of heat transfer in a turbulent flow in channels with gap". *Eng. Térmica*, Vol. 13, pp. 96–103.

Wu, X. and Trupp, A.C., 1993. "Experimental study on the unusual turbulence intensity distributions in rod-to-wall gap regions". *Exp. Thermal Fluid Sci*, Vol. 6, pp. 360 – 370.

Wu, X. and Trupp, A.C., 1994. "Spectral measurements and mixing correlation in simulated rod bundle subchannels." *Int.J.Heat Mass Transfer*, Vol. 37, pp. 1277 – 1281.

9. RESPONSIBILITY NOTICE

The author are the only responsible for the printed material included in this paper.